Materials Science & Engineering A 680 (2017) 411–420

Contents lists available at ScienceDirect

Materials Science & Engineering A

journal homepage: www.elsevier.com/locate/msea

Crashworthiness of graded cellular materials: A design strategy based on a nonlinear plastic shock model

Jie Yang, Shilong Wang, Yuanyuan Ding, Zhijun Zheng*, Jilin Yu

CAS Key Laboratory of Mechanical Behavior and Design of Materials, University of Science and Technology of China, Hefei 230026, PR China

ARTICLE INFO

Keywords:
Graded cellular materials
Crashworthiness
Density design
R-PH idealization
Shock model
Finite element method

ABSTRACT

Dynamic behaviors and crashworthiness design of density graded cellular materials are investigated by using theoretical method and finite element simulation. A nonlinear plastic shock model is employed to guide the gradient design of cellular rod under mass impact and cell-based finite element models are used to verify the design strategy. Effects of impact-force parameter on the design of relative density distribution of graded cellular material and on the residual velocity of the striker for different lengths of graded cellular rods are explored. Three cases of design strategy with different impact-force parameters are analyzed and verified. The results reveal that the design strategy is reliable when the impact-force parameter is not less than zero. If the relative density distribution of graded cellular rod increases monotonically, the actual deformation mode of graded cellular rod is identical with the assumed one in the theoretical derivations. It is noticed that a portion of the graded cellular rods close to the distal end is not fully compacted. A scheme with restricting the shock strain not less than a specific value is proposed to shorten the graded cellular rods. Therefore, the desirable crashworthiness of graded cellular materials can be obtained by designing the density distribution of graded cellular materials.

1. Introduction

Cellular materials may improve the crashworthiness of structures used in automotive, railway and aeronautical industries [1,2]. Under quasi-static loading rates, the nominal stress-strain curves of cellular material present three distinct deformation stages, namely elastic, long plateau and densification stages [3]. Under high loading rates, the dynamic behaviors of cellular material can be featured by stress enhancement and deformation localization [4–6]. The typical feature of strength enhancement can improve the capacity of energy absorption of cellular materials. Introducing a density gradient to cellular materials may further improve their dynamic mechanical properties [7,8].

The dynamic features of cellular materials are resulted from inertia [5], as explored in shock models [9–16]. Several idealizations of cellular materials have been proposed to develop shock models [9–16]. A rate-independent, rigid–perfect plastic–locking (R-PP-L) idealization was first introduced by Reid and Peng [9] to develop a shock model and explain the dynamic behavior of wood. This model was further applied to investigate the dynamic behavior of metal foams by Tan et al. [10]. Recently, Zheng et al. [15,16] introduced a rate-independent, rigid–plastic hardening (R-PH) idealization to describe the uniaxial compression behavior of uniform cellular materials, in which the stress–strain relation is expressed as

$$\sigma(\varepsilon) = \sigma_0 + \frac{C\varepsilon}{(1-\varepsilon)^2}, \tag{1}$$

where σ_0 is the initial crushing stress and C the strain hardening parameter. The R-PH shock model was then developed by Ding et al. [17] to investigate the anti-blast behavior of cellular sacrificial cladding. An asymptotic solution of critical length was proposed to guide the design of cellular sacrificial cladding, which shows a good agreement with the finite element (FE) results.

Graded cellular materials have been widely investigated due to their considerable capacity of impact resistance and energy absorption. Researches have showed that a density gradient has significant influence on the mechanical response of cellular materials under quasi-static compression [18,19]. Dynamic response of graded cellular materials revealed that a density gradient could improve the energy absorption capacity [20,21]. Due to the limitations of material fabrication technology, some density-graded open-/closed-cell foam specimens were manufactured by using adhesive technique [22–25], which integrates graded cellular materials by bonding different densities foam layers. Experimental results may be affected by the complicated stress

* Corresponding author.
E-mail address: zjzheng@ustc.edu.cn (Z. Zheng).

http://dx.doi.org/10.1016/j.msea.2016.11.010
Received 9 October 2016; Received in revised form 31 October 2016; Accepted 5 November 2016
Available online 09 November 2016

wave transmission and reflection occurring at the interface between layers [23,25]. As graded cellular specimens with a specific relative density distribution are not yet easily obtained in practical application, many researchers turn to apply FE methods [7,21] and shock models [8,20] to study the mechanical responses of graded cellular materials with different relative density distributions.

Investigations based on the stress wave theory and FE method were performed to reveal the mechanism of deformation and energy absorption of graded cellular metals and to estimate the energy absorption capability and impact resistance. Results indicated that a density gradient can influence stress waves in the graded cellular materials during impact [26,27] and reduce the maximum impact stress for the protected structures [28]. Three deformation modes of graded cellular materials under impact loading were found and analyzed [21], and it was found that graded cellular metals with a specific density gradient could improve the performance of energy absorption and impact resistance for different protected objects [29–32]. However, most researches in the literature [7,21,30,33] were focused on the dynamic responses of graded cellular materials with a specific relative density distribution, but few on the crashworthiness design [31,32]. Wang et al. [31] investigated the optimal density-gradient parameters of graded cellular metals with a linear density gradient of different average relative densities to meet the crashworthiness requirements of high energy absorption, stable impact resistance and low peak stress. Thus, the applicable potential of cellular materials in crashworthiness structures may be enhanced by developing crashworthiness design methods.

This study aims to propose a method for guiding the crashworthiness design of graded cellular material and to obtain the desirable crashworthiness property. Based on the R-PH shock model, a design strategy to determining the relative density distribution of graded cellular material for specific crashworthiness requirements is presented in Section 2. An FE method using 3D Voronoi models with specific relative density distributions of graded cellular material is introduced also in Section 2. Influences of an impact-force parameter on the crashworthiness and relative density distributions of graded cellular rods are analyzed in Section 3. Three cases of mass impact with specific impact forces are investigated by using the shock model and verified by the FE method also in Section 3. Conclusions are given in Section 4.

2. Theoretical and numerical models

2.1. Problem description

We consider an object with mass M and initial velocity V_0 impinging a graded cellular rod at time t=0. The object is to be protected, which requires that the impact force acting on the object should be less than that the object can bear. Thus, the graded cellular rod needs a suitable design to satisfy the requirement for protecting the object. In many practical applications, a stable impact force is desirable, i.e. the impact force keeps constant. In some applications, multiple energy absorber elements may be used in a crashworthy system, which is triggered under different values of impact forces, and the design without a step of impact force [34] may be desirable, i.e. the impact force increases gradually. In some other applications, the design may take the tolerable intensity of human body into consideration. For example, as illustrated in Wayne Tolerance Curve [35], the tolerable intensity of human body decreases as the time of exposure to pressure increases, and thus a decreasing history of impact force may be desirable. Therefore, the desirable impact force acting on the object may be very different in applications. For simplicity, we consider the case that the impact force varying with time in a linear manner, written as

$$F(t) = [1 + \alpha(t/T - 1/2)]F_0, \tag{2}$$

where α is an impact-force parameter, T the impact duration, F_0 the impact force at time $T/2$. In the design, the object can be taken as a rigid mass. Then, the relative density distribution of the graded cellular rod, denoted as $\rho(X)$ along the X-axis direction, may be determined with the help of analyzing a shock model.

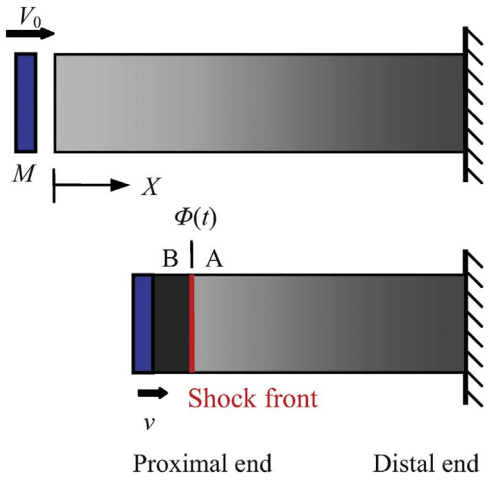

Fig. 1. Mass impact of graded cellular rod and a shock model.

Assuming there is one shock front propagating from the proximal end to the distal end of the graded cellular rod, as presented schematically in Fig. 1. Indeed, this implies that the relative density distribution $\rho(X)$ is a non-decreasing monotonic function [31]. During crushing, the portion behind the shock front moves together with the mass, while the portion ahead of the shock front is stationary. The physical quantities, including strain, stress and particle velocity, behind the shock front are denoted as $\{\varepsilon_B(t), \sigma_B(t), v(t)\}$; while those ahead of the shock front are $\{0, \sigma_A(t), 0\}$. Hereafter, the strain (stress) behind the shock front is named as the shock strain (stress). Thus, according to Newton's motion law, the acceleration of the portion behind the shock front at time t can be given by

$$a(t) \equiv \frac{dv(t)}{dt} = -\frac{A_0\sigma_B(t)}{M + A_0\rho_s\int_0^{\Phi(t)}\rho(X)dX}, \tag{3}$$

where $\Phi(t)$ is the Lagrangian location of the shock front, A_0 the cross-sectional area of the graded cellular rod, and ρ_s the density of matrix material of the graded cellular rod. On the other hand, if the impact force $F(t)$ is specified, e.g. Eq. (2), the acceleration of the mass can be calculated by

$$a(t) = -F(t)/M. \tag{4}$$

From Eqs. (3) and (4), it can be concluded that the impact force is highly dependent on the relative density distribution of graded cellular rod. Thus, the impact resistance performance of graded cellular rod can be improved with a reasonable design of its density distribution. Combining Eqs. (3) and (4), we have the shock stress

$$\sigma_B(t) = \left(1 + \frac{\rho_s A_0}{M}\int_0^{\Phi(t)}\rho(X)dX\right)\cdot\frac{F(t)}{A_0}. \tag{5}$$

Then, with using a material model of the graded cellular rod, we can determine the relative density distribution, as illustrated in the next section. In this study, we take M =50 g, V_0 =100 m/s and F_0 =7.5 kN with different values of parameter α as study cases to demonstrate our design strategy. The impact duration T can be obtained from the impulse-momentum theorem, i.e. $\int_0^T F(t)dt = MV_0$ gives T=0.67 ms.

2.2. Nonlinear plastic shock model

A design strategy based on a nonlinear plastic shock model is proposed to determine the relative density distribution of graded cellular rod. Instead of the R-PP-L idealization [9,31], a more accurate

material model, e.g. the R-PH idealization [16], is employed here to characterize the stress–strain relation of cellular materials, see Eq. (1). For a specific density distribution of specimen, the two material parameters of the R-PH idealization, namely the initial crushing stress and the strain hardening parameter, are both related to the local density distribution. These two material parameters may be expressed in power-law forms, written as

$$\left.\begin{aligned}\sigma_0(\rho) &= \sigma_{ys}\cdot k_1\rho^{n_1}\\ C(\rho) &= \sigma_{ys}\cdot k_2\rho^{n_2}\end{aligned}\right\}, \tag{6}$$

where σ_{ys} is the yield stress of matrix material, k_1, k_2, n_1 and n_2 are material parameters which can be obtained by fitting the nominal stress-strain curves of cellular materials with different densities under quasi-static compression, see Section 2.3. For the shock model based on this R-PH idealization, the stress ahead of the shock front is given by $\sigma_A(t) = \sigma_0(\rho)$ and the shock stress can be expressed as

$$\sigma_B(t) = \sigma_0(\rho) + \frac{C(\rho)\varepsilon_B(t)}{(1-\varepsilon_B(t))^2}. \tag{7}$$

The basic equations to determine the relative density distribution can be obtained from this nonlinear plastic shock model, see Appendix A for the derivations. Thus, from Eqs. (A.6), (A.8) and (4), we have the basic equations

$$\begin{cases}\dfrac{d\rho(\Phi(t))}{dt} = \dfrac{F^2(t)\rho_s\rho(3v+2c(\rho))+\dot{F}(t)M[\sigma_0(\rho)+\rho\rho_s v(v+c(\rho))]}{F(t)M[\sigma_0'(\rho)+\rho_s v^2+\rho_s v(c(\rho)+\rho c'(\rho))]}\\ \dfrac{d\Phi(t)}{dt} = v(t)+c(\rho)\\ \dfrac{dv(t)}{dt} = -\dfrac{F(t)}{M}\end{cases} \tag{8}$$

with $c(\rho) = \sqrt{C(\rho)/(\rho\rho_s)}$, where the overdot and apostrophe represent the derivatives with respect to t and ρ, respectively. A fourth-order Runge-Kutta scheme was employed to solve Eq. (8) with a given impact force history $F(t)$ and the initial conditions $\Phi(0)$ =0, $v(0) = V_0$ and $\rho(\Phi(0)) = \rho_0$, where ρ_0 can be determined from Eq. (A.9), i.e.

$$\sigma_0(\rho_0) + \rho_0\rho_s V_0(V_0 + c(\rho_0)) = F(0)/A_0, \tag{9}$$

with applying numerical analysis, e.g. Newton's method.

2.3. Cell-based finite element model

A varying cell-size distribution method based on Voronoi technique has been developed to construct 2D graded cellular structures [31,36]. In this study, we extended this method to construct 3D graded cellular structures and then used them to verify the design strategy based on the shock model. Closed-cell foam models with uniform density distributions have been generated by applying the 3D Voronoi technique, see Ref. [16] for details. Here, a new principle of random seeding nuclei is proposed, i.e. the distance between any two nuclei i and j is required to be

$$\delta_{ij} \geq (1-k)\delta_{\min}(\rho_{ij}) = (1-k)\cdot\frac{3(6+\sqrt{3})h}{8\rho_{ij}}, \tag{10}$$

where k is the cell irregularity, $\delta_{\min}(\rho)$ the minimum distance of any two adjacent nuclei in a tetrakaidecahedron structure with relative density ρ, ρ_{ij} the local relative density at the middle point between any two nuclei i and j, and h the cell-wall thickness. With this new principle, density-graded cellular structures can be constructed for a given distribution of relative density. A sample is illustrated in Fig. 2(a). In this study, we take k=0.4 and h =0.20 mm.

Mass impact tests are performed by using FE method with ABAQUS/Explicit code. Rectangular specimens are hold behind a stationary platen and impacted by a rigid platen with mass M and initial velocity V_0 along the longitudinal direction, as presented schematically in Fig. 2(b). During the uniaxial loading, the transverse directions of the specimens are free. The cell-wall material is taken to be elastic-perfectly plastic and the parameters of matrix material, including density, Young's modulus, Possion's ratio and yield stress, are set as ρ_s =2700 kg/m^3, E =69 GPa, ν=0.3 and σ_{ys} =165 MPa, respectively. Cell walls are meshed with hybrid shell elements of type S3R. Through a mesh sensitivity study [16], the characteristic size of shell elements is set to be about 0.3 mm. The cross section of specimens has a size of 30 mm×30 mm. A general contact interaction with a friction coefficient of 0.02 is applied to all possible contact surfaces [16]. One calculation step is applied with a duration of 0.8 ms and the time step is automatically adjusted.

To determine the parameters in Eq. (6), closed-cell foam models with uniform density distributions are generated as in Ref. [16] and loaded in a uniaxial constant-velocity compression scenario at a velocity of 10 m/s. Samples are generated in a volume of 20×20×30 mm^3 with 600 nuclei and k=0.4. Typical nominal stress–strain relations for different relative densities are presented in Fig. 3(a). By fitting the curves with Eq. (1), the initial crush stress and the strain hardening parameter for different relative densities are obtained, see Fig. 3(b). Then, fitting the data in Fig. 3 by Eq. (6) yields k_1 =0.885, n_1 =1.37, k_2 =0.115 and n_2 =1.50.

3. Results and discussion

3.1. Gradient design based on the shock model

For the impact force linearly varying with time described by Eq. (2), a positive value of α gives an increasing impact-force history, while a negative value of α presents a decreasing impact-force history. A large value of α corresponds to a small value of the impact force at the start of impact. Thus, one may expect a small relative density at the proximal end of the graded cellular rod to achieve a large value of α, as shown in Fig. 4, which is determined from Eq. (9). Three values of impact-force parameter α, namely α=0, 2/3 and −2/3, are considered and the corresponding relative density distributions of graded cellular rods can be determined from Eq. (8), as shown in Fig. 5. We employ a cubic function to fit the relative density distributions, written as

$$\rho(X) = b_0 + b_1(X/L_0) + b_2(X/L_0)^2 + b_3(X/L_0)^3, \tag{11}$$

where L_0 is the length of the graded cellular rod that is just enough to absorb all the kinetic energy of the whole system and b_i (i=0, 1, 2, 3) are fitting parameters. The values of these parameters corresponding to different values of α are given in Table 1. These results show that a large value of α leads to a large value of L_0. It is noticed that for α=−2/3, the relative density distribution $\rho(X)$ is not an increasing monotonic function. This is conflict with the assumption of the shock model, i.e. $\rho(X)$ is a non-decreasing monotonic function and only one shock front propagates in the rod.

From the shock model, if the length of the graded cellular rod is restricted, the kinetic energy of the system may not be absorbed completely at the time when the shock front arrives at the distal end, and the object may still have a finite velocity, which is defined here as the theoretical residual velocity of the object and denoted as V_r. For $-2 < \alpha < 2$, if the length of the graded cellular rod L is larger than 76 mm, all the kinetic energy of the system can be fully absorbed by the rod. For a given value of L, the residual velocity V_r increases with the increase of α, as shown in Fig. 6. In Fig. 6, curve AB represents $L = L_0$ for different α. In Region I, the shock model predicts an increasing relative density distribution, but in Region II, the shock model predicts a decreasing relative density distribution, which may fail to present a correct guide. Nevertheless, this flaw of the shock model may not lead to significant error. According to the shock model, the shock strain of cellular material depends on the relative density and the impact velocity, see Eq. (A4). When the impact velocity is small enough, the shock strain is small too and the cellular material close to the distal end may not be compacted fully, i.e. it still has a capacity to absorb more energy.

To verify our design strategy, numerical simulations using cell-

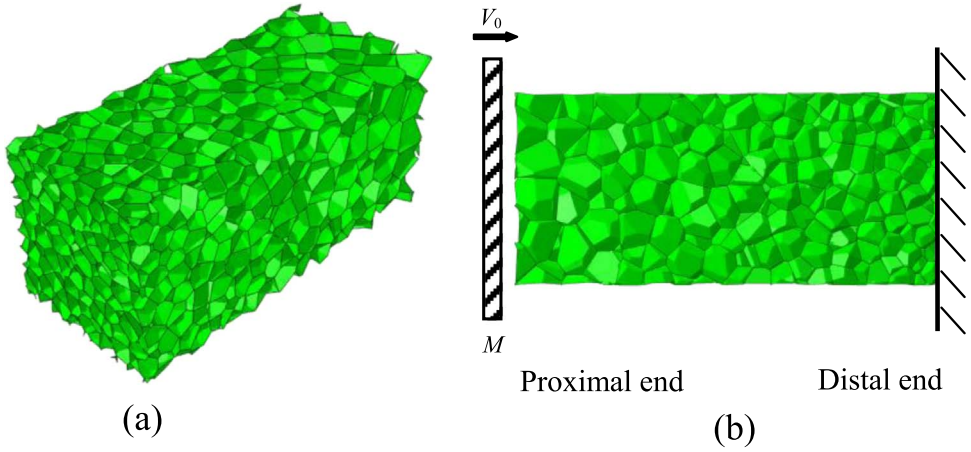

Fig. 2. Illustrations of (a) a specimen of density graded cellular structure and (b) a mass impact test with 3D Voronoi model.

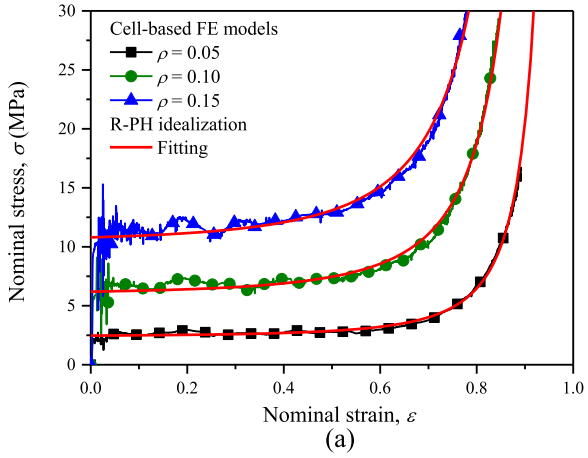

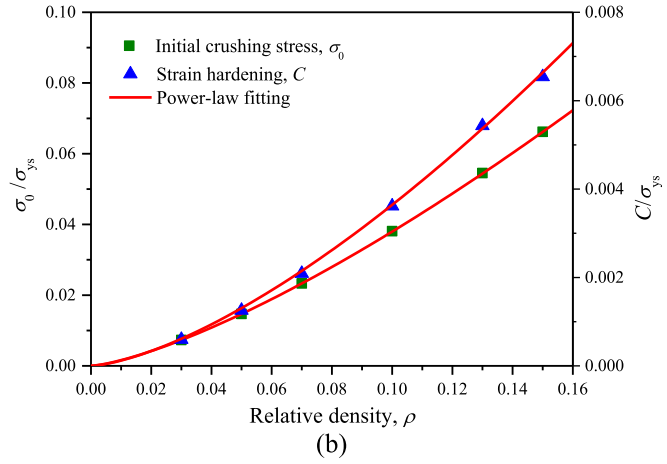

Fig. 3. (a) Nominal stress–strain relations for different relative densities and (b) fitting results of parameters in the R-PH idealization.

based FE models for the cases of α=0, 2/3 and −2/3 are carried out in the next section.

3.2. Verification by numerical simulations

3.2.1. Case 1: a constant impact force

For the case of α=0, a constant impact force is set as the design objective. According to the relative density distribution presented above, a cell-based FE model with length $L = L_0$ =66.3 mm is generated, see Fig. 7(a). Deformation patterns of this specimen are

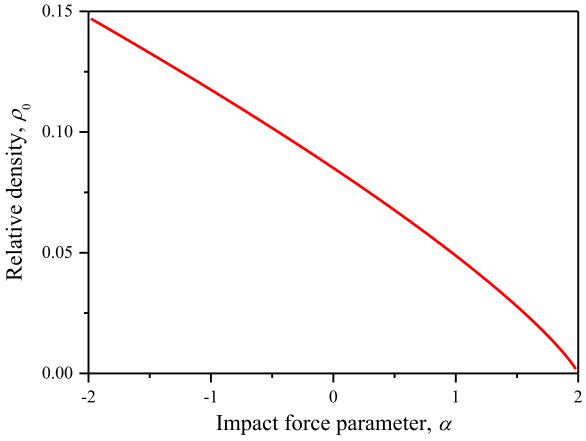

Fig. 4. Variation of the relative density at proximal end, ρ_0, with the impact-force parameter α.

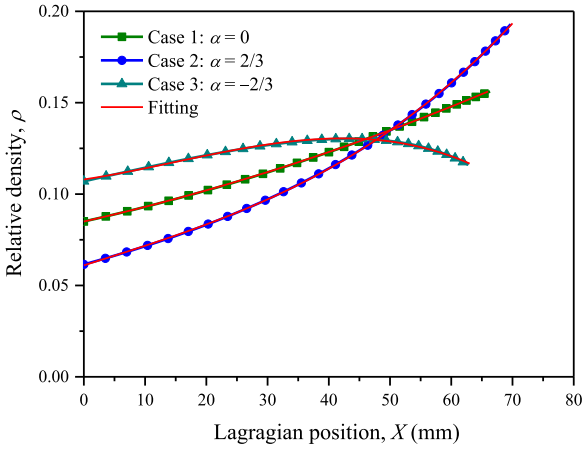

Fig. 5. Relative density distributions and fitting results for three values of the impact-force parameter α.

Table 1
Values of L_0 and fitting parameters in Eq. (11) for different impact-force parameters.

α	L_0 (mm)	b_0	b_1	b_2	b_3
−2/3	62.8	0.108	0.0307	0.0550	−0.0780
0	66.3	0.0850	0.0498	0.0213	0
2/3	69.7	0.0610	0.0742	−0.00279	0.0610

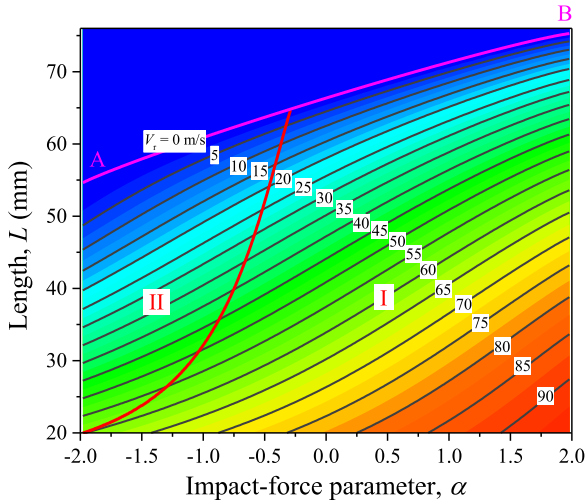

Fig. 6. A contour map of the residual velocity for the different impact-force parameters and different lengths of graded cellular rod.

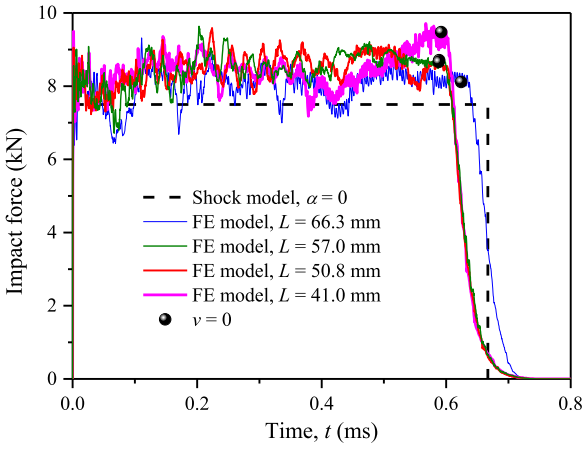

Fig. 8. Comparison of impact forces obtained from the shock model and the cell-based FE model in the case of α=0.

presented also in Fig. 7(a). It is observed that the crushing band propagates from the proximal end to the distal end. As the relative density of the cellular material close to the proximal end is lower than the one close to the distal end and there is an increasing distribution of the initial crush stress along the graded cellular rod, the cellular material ahead of the shock front deforms in an elastic manner. A comparison of the impact force history curves between the theoretical prediction and the FE result is shown in Fig. 8. The fluctuation of the

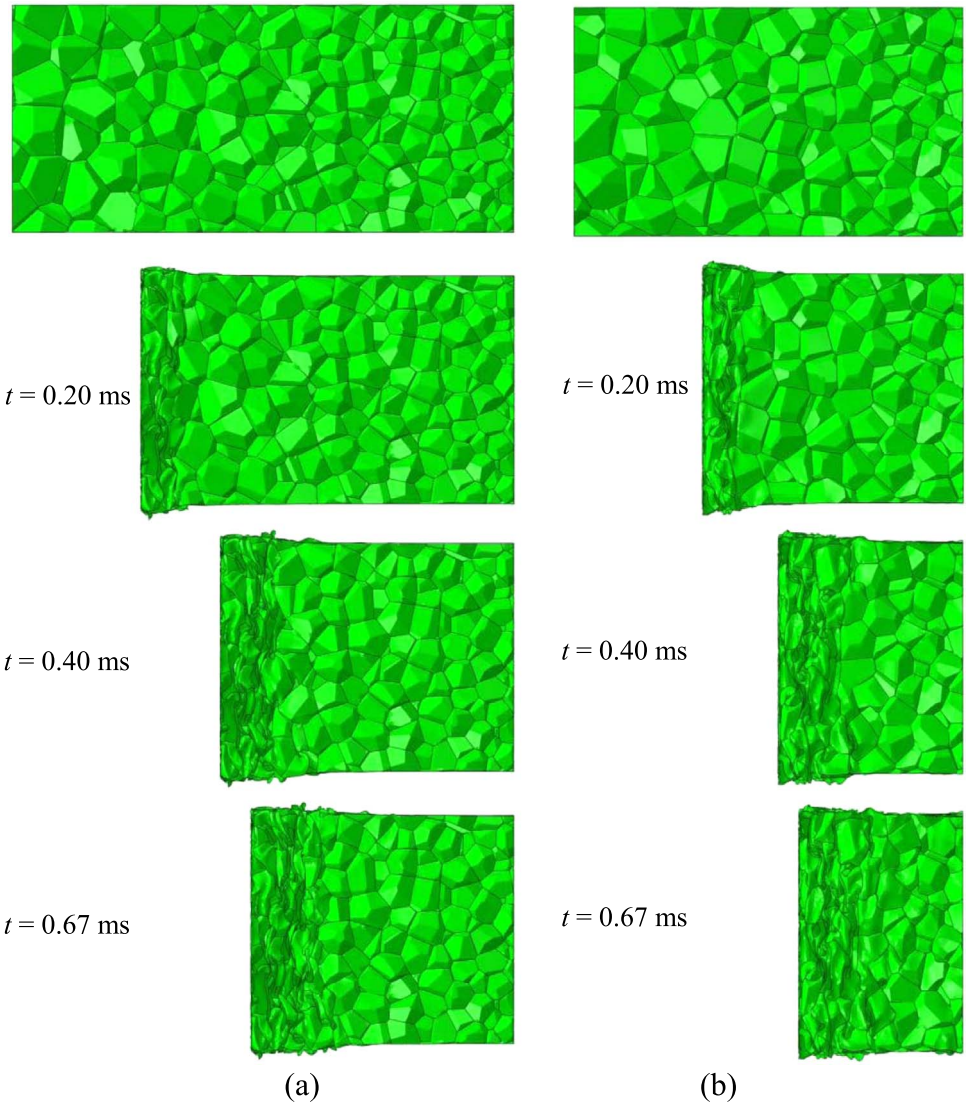

Fig. 7. Deformation patterns in the case of α=0 with different lengths: (a) L =66.3 mm, (b) L =50.8 mm.

FE result is mainly due to the collapse of cells and the propagation of elastic waves. After impact, the object is rebounded with a low velocity due to the releasing of the elastic energy of cellular material. The average value of the impact force obtained from the cell-based FE model is a little greater than the value of the theoretical prediction. The possible reason is that the rate sensitivity of cellular material is not considered in the shock model, i.e. the initial crushing stress and the strain hardening parameter are determined from the quasi-static compressive stress–strain curves, see Fig. 3. Recent researches [16,37] show that the local stress–strain behavior of cellular material under high-velocity impact is very different from the quasi-static compressive stress–strain curve, i.e. the constitutive behavior of cellular material is rate-sensitive. In further study, the design strategy may be refined with considering the rate sensitivity of cellular material. From Fig. 7(a), we noticed that the cells close to the distal end are not fully collapsed at the end of impact. Thus, the length of the graded cellular rod may be shortened to improve the design strategy, as discussed below.

From Fig. 7(a), nearly 30% of the specimen is almost undeformed in the FE simulation. This means the specimen is not compacted fully and the design strategy based on the R-PH idealization presented above may be conservative. As the strain hardening of cellular material is considered in the R-PH shock model (different to the R-PP-L shock model), the shock strain may be less than the densification strain of cellular material when the impact velocity is small enough, as illustrated in Eq. (A.4) and shown in Fig. 9. With the decrease of the impact velocity, the shock stress is reduced but the stress wave still propagates in the cellular material. When the shock front arrives at the distal end, the strain of the cells close to the distal end is quite smaller than the densification strain of cellular material and the cellular material close to the distal end is far from being fully utilized. Thus, if we restrict the shock strain at the distal end to an appropriate value, the graded cellular rod can be shortened and the impact force may still satisfy the requirement. Here, an improved design strategy with restricting the shock strain at the distal end is proposed to shorten the graded cellular rod. We consider the shock strain at the distal end to be 0.5, 0.4 or 0.3 when the shock front arrives at the distal end. Then, the length of the cellular rods, L, can be shortened as 41.0 mm, 50.8 mm or 57.0 mm, as illustrated in Fig. 9. In this study, the compaction strain of cellular materials with relative density less than 0.2 is larger than 0.5 [2] and thus the shortened graded cellular rods still have energy absorption capability after the shock front arrives at the distal end. Cell-based FE simulations for the shortened rods have been carried out and a comparison of the impact forces is shown in Fig. 8. For the three cases of shortened rods, the levels of impact force do not change much, and only for the case of L =41.0 mm, the impact

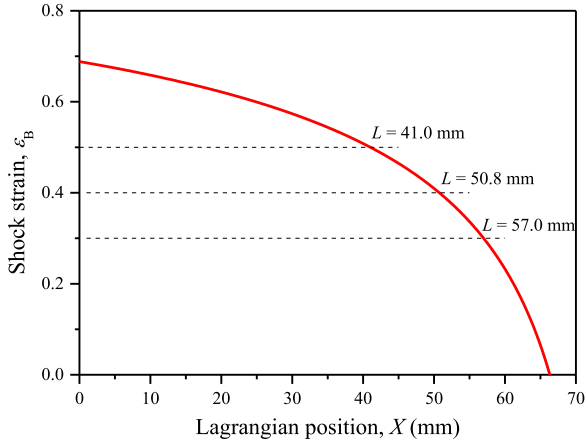

Fig. 9. The shock strain at different Lagrangian positions at the end of the impact.

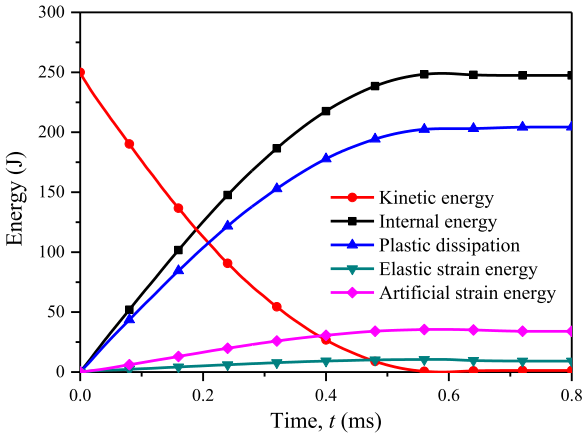

Fig. 10. Energy absorption curves in the case of α=0 with length L =50.8 mm.

force rises to a great value after t=0.4 ms. Apparently, the case of L =57.0 mm has a lower utilization rate than the case of L =50.8 mm. Thus, restricting the shock strain at the distal end to be 0.4 seems much appropriate and it is suggested as an improved design strategy. Here, the strain value of 0.4 is empirical. With this improved design strategy, a reduction of 23.4% in the length of graded cellular rod is achieved. Deformation patterns for the improved design strategy are shown in Fig. 7(b). It shows that the deformation mode is the same as the original case, but the un-compacted portion becomes shorter. The energy absorption curves for the improved design strategy are plotted in Fig. 10. It shows that the kinetic energy of the object decreases to zero and most of kinetic energy is absorbed by the graded cellular rod in the form of plastic dissipation.

3.2.2. Case 2: an increasing impact force

The 3D Voronoi specimen with a relative density distribution corresponding to the case of α=2/3 with length $L = L_0$ =69.7 mm is shown in Fig. 11(a). As the relative density also increases monotonically from the proximal to the distal end, the cellular material is crushed from the proximal end to the distal end, as shown in Fig. 11(a). The specimen is also not fully compacted for the same reason mentioned above. The impact force history obtained by the FE simulation is compared with the set one, as shown in Fig. 12. The impact force has an increasing trend and fluctuates near the force value set in the shock model as the cells collapse during the impact. This result shows the force obtained by cell-based FE model is in good agreement with the set value in the shock model. Thus, this design scheme is proven to be reliable.

Similar to Case 1, the cells close to the distal end are not collapsed after impact and the graded cellular rod in Case 2 can also be shortened, see Fig. 11(a). By restricting the shock strain not less than 0.4, the length of the graded cellular rod can be determined to be 56.3 mm by using the shock model, which has a reduction of 19.2%. Cell-based FE simulation for this shortened rod is carried out and the deformation patterns are shown in Fig. 11(b). It shows that some cells close to the distal end have slight deformation, but they still have energy absorption capacity after impact. The impact force history for this shortened rod is presented also in Fig. 12. Before time 0.5 ms, the impact force of the shortened rod is close to that of the original rod, but subsequently, the values of impact force are slightly larger than those of the original rod.

3.2.3. Case 3: a decreasing impact force

A 3D Voronoi specimen with the relative density distribution corresponding to the case of α=−2/3 with length $L = L_0$ =62.8 mm is generated, see Fig. 13(a). With the variation of Lagrangian position X, the relative density increases at first and then decreases, as shown in Fig. 5. Deformation patterns are shown in Fig. 13(a) and a comparison

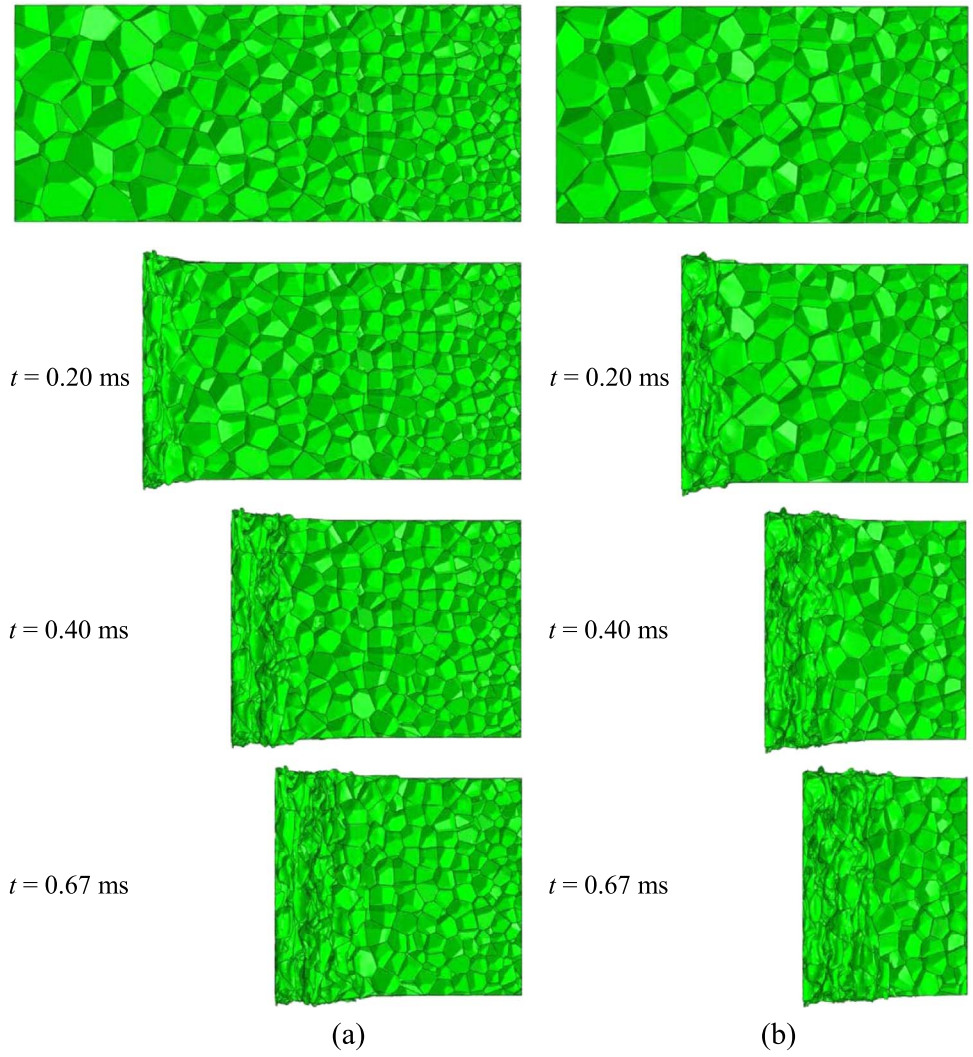

Fig. 11. Deformation patterns in the case of α=2/3 with different lengths: (a) L =69.7 mm, (b) L =56.3 mm.

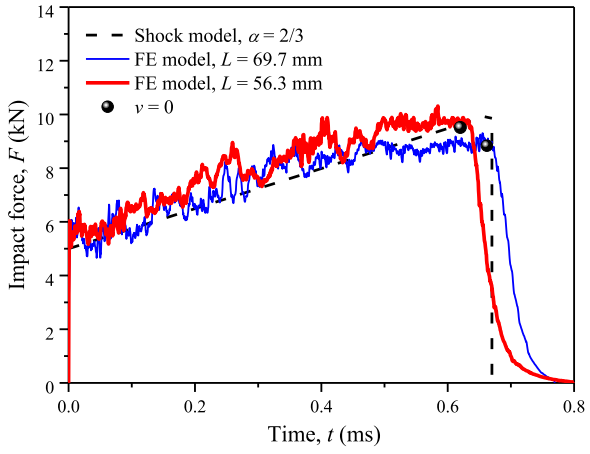

Fig. 12. Comparison of impact forces obtained from the shock model and the cell-based FE model in the case of α=2/3.

of impact force history curves between the two models is shown in Fig. 14. As the relative density distribution is not an increasing monotonic function, the cellular material close to the distal end is also deformed during impact, see Fig. 13(a). The values of impact force obtained by the cell-based FE model are larger than the theoretical ones and the impact duration is shorter than the theoretical prediction, as shown in Fig. 14. Obviously, the design scheme of this case is conflict between the shock model and the cell-based model. The actual propagation of shock front for this case is different from the assumed one in the theoretical derivations. Actually, two shock fronts appear at the both ends of the specimen and thus the theoretical derivation in Appendix A is not applicable for this case.

In the shock model, by restricting the shock strain at the distal end to be 0.4, the graded cellular rod is shortened to be 45.0 mm, which has a reduction of 28.3% in length. According to Fig. 5, the relative density distribution of the case α=−2/3 is almost in an increasing manner when X < 45 mm. A cell-based FE simulation is performed to investigate the crashworthiness of this graded cellular rod. Deformation patterns of this shortened rod are shown in Fig. 13(b) and the impact force history obtained from the cell-based FE model is presented in Fig. 14. During impact, crushing bands appear first at the proximal end of the cellular rod and a shock front propagates to the distal end, but after time 0.30 ms, the cellular material close to the distal end is deformed. The relative density in the region close to the distal end changes little, see Fig. 5, and thus the corresponding strength of cellular material does not have apparent change. But, the cutting imperfections may soften the strength of incomplete cells at the distal end [38]. The value of the impact force obtained by the cell-based FE model with L =45.0 mm approximately equals to the values of that with L =62.8 mm when t < 0.4 ms.

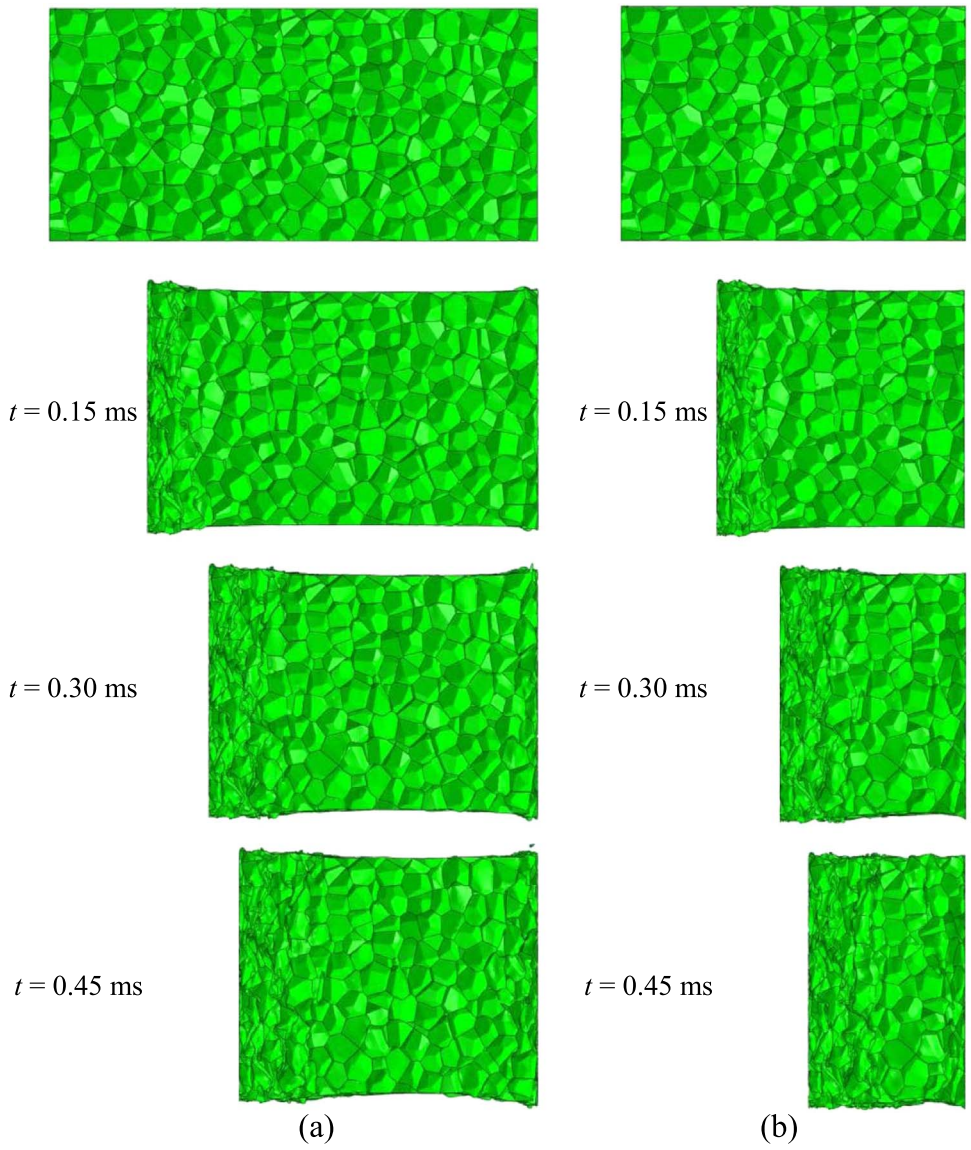

Fig. 13. Deformation patterns in the case of α=−2/3 with different lengths: (a) L =62.8 mm, (b) L =45.0 mm.

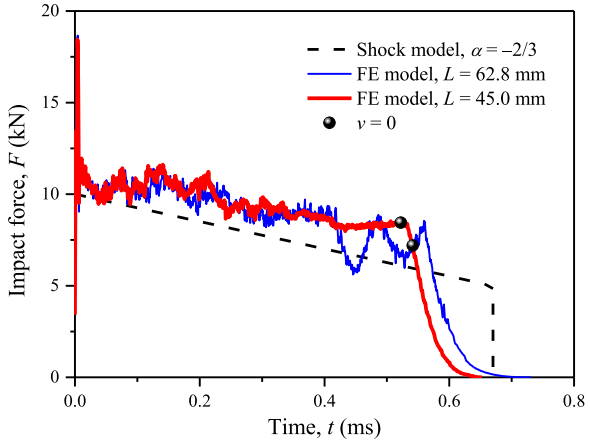

Fig. 14. Comparison of impact forces obtained from the shock model and the cell-based FE model in the case of α=−2/3.

4. Conclusions

A nonlinear plastic shock model based on the R-PH idealization is employed to guide the gradient design of graded cellular rods. Differential equations are obtained to determine the relative density distribution of graded cellular rod. Cell-based FE models for graded cellular rods are constructed and used to verify the design strategy.

A linearly-varying impact force history is considered as the design strategy of crashworthiness in this study. It is found that the relative density at the proximal end of graded cellular rod decreases with the increase of the impact-force parameter. Based on the R-PH shock model, we evaluated the theoretical residual velocity of the protected object when the length of graded cellular rod is restricted. The single shock model shows that the theoretical residual velocity of the protected object increases with the increase of the impact-force parameter. But, it should be noticed that (1) the single shock model may be not available for the cases of the impact-force parameter being less than zero and (2) there is not necessarily a residual velocity for a cell-based FE model or a practical specimen.

Three cases of different impact force requirements are investigated and analyzed. Based on the R-PH shock model, the relative density distribution of α=0 or 2/3 is monotonically increasing, but that of

α=−2/3 increases at first and then decreases. It can be deduced that relative density distribution would be an increasing monotonic function for the cases of α not less than zero, which confirms to the assumption of one shock front in the theoretical derivations. 3D Voronoi models are generated and their mass-impact responses are simulated by using the FE code ABAQUS/Explicit. Results of impact force and the impact force at the distal end obtained from the cell-based FE models are in good agreement with those of the shock models for the cases of α=0 and 2/3, but not for α=−2/3. For the case of α=−2/3, it is found that deformations appear at both ends in the graded cellular rod and this is conflict with the assumption in the theoretical derivations. These results show that when the actual deformation mode conforms to the theoretical assumption, the crashworthiness of density graded cellular materials can be design accurately.

As shown in the deformation patterns, the un-compacted portions indicate that the original designs are conservative and the design strategy can be improved. Graded cellular rods can be shortened by restricting the shock strain at the distal end when the shock front arrives at the distal end. The dynamic behaviors of the shortened rods are also investigated by using the cell-based FE models. Results show that the improved design strategy has a greater utilization rate in materials than the original one. In further study, the hardening behavior of the matrix material, which can affect the initial crushing stress and the strain hardening parameter of cellular material [37], the rate sensitivity of cellular materials [16] may be considered to improve the precision of the crashworthiness design and the related work can be extended to investigate different loading scenarios and different design objectives.

Acknowledgements

This work is supported by the National Natural Science Foundation of China (Projects Nos. 11372308 and 11372307) and the Fundamental Research Funds for the Central Universities (Grant No. WK2480000001).

Appendix A. Derivations of the nonlinear plastic shock model

According to stress wave theory [39], the conservation conditions of mass and momentum across the shock front give

$$v(t) - 0 = \dot{\Phi}(t)(\varepsilon_B(t) - 0) \tag{A.1}$$

and

$$\sigma_B(t) - \sigma_0(\rho) = \rho\rho_s\dot{\Phi}(t)(v(t) - 0), \tag{A.2}$$

respectively, where $\dot{\Phi}(t)$ is the shock wave speed. Eliminating $\dot{\Phi}(t)$ from Eqs. (A.1) and (A.2) leads to

$$\sigma_B(t) = \sigma_0(\rho) + \frac{\rho\rho_s v^2(t)}{\varepsilon_B(t)}. \tag{A.3}$$

This relation is consistent with that of the shock models for uniform cellular materials [9], but here the relative density is related to the Lagrangian position, i.e. ρ= $\rho(\Phi(t))$. Combining Eqs. (A.3) and (7), we have the shock strain

$$\varepsilon_B(t) = \frac{v(t)}{v(t) + c(\rho)} \tag{A.4}$$

and the shock stress

$$\sigma_B(t) = \sigma_0(\rho) + \rho\rho_s v(t)(v(t) + c(\rho)), \tag{A.5}$$

where $c(\rho) = \sqrt{C(\rho)/(\rho\rho_s)}$ is the difference between the shock wave speed and the impact velocity, as implied in Eqs. (A.1) and (A.4). Thus, the stress wave speed can be written as

$$\dot{\Phi}(t) = v(t) + c(\rho). \tag{A.6}$$

Combining Eqs. (5) and (A.5) leads to

$$1 + \frac{\rho_s A_0}{M}\int_0^{\Phi(t)} \rho(X)dX = \frac{A_0}{F(t)}[\sigma_0(\rho) + \rho\rho_s v(t)(v(t) + c(\rho))]. \tag{A.7}$$

Differentiating both sides of Eq. (A.7) with respect to t, we get

$$\frac{d\rho}{dt} = \frac{F^2(t)\rho_s\rho(\dot{\Phi}(t) + 2v + c(\rho)) + \dot{F}(t)M[\sigma_0(\rho) + \rho\rho_s v(v + c(\rho))]}{F(t)M[\sigma'_0(\rho) + \rho_s v(v + c(\rho)) + \rho\rho_s vc'(\rho)]}. \tag{A.8}$$

At the beginning of impact, $\Phi(0)$ =0 and $v(0) = V_0$, and thus from Eq. (A.7) we have

$$\sigma_0(\rho(0)) + \rho(0)\rho_s V_0(V_0 + c(\rho(0))) = F(0)/A_0, \tag{A.9}$$

which gives the relative density at the proximal end, i.e. $\rho(0) = \rho_0$.

References

[1] L.J. Gibson, M.F. Ashby, Cellular Solids: Structure and Properties, Cambridge University Press, 1997.
[2] M.F. Ashby, T. Evans, N. Fleck, L.J. Gibson, J.W. Hutchinson, H.N.G. Wadley, Metal foams: a design guide, Elsevier Sci. (2000).
[3] L.J. Gibson, Mechanical behavior of metallic foams, Annu. Rev. Mater. Sci. 30 (1) (2000) 191–227.
[4] Z.J. Zheng, J.L. Yu, J.R. Li, Dynamic crushing of 2D cellular structures: a finite element study, Int. J. Impact Eng. 32 (1–4) (2005) 650–664.
[5] Y.D. Liu, J.L. Yu, Z.J. Zheng, J.R. Li, A numerical study on the rate sensitivity of cellular metals, Int. J. Solids Struct. 46 (22–23) (2009) 3988–3998.
[6] I. Elnasri, S. Pattofatto, H. Zhao, H. Tsitsiris, F. Hild, Y. Girard, Shock enhancement of cellular structures under impact loading: part I experiments, J. Mech. Phys. Solids 55 (12) (2007) 2652–2671.

[7] A. Ajdari, P. Canavan, H. Nayeb-Hashemi, G. Warner, Mechanical properties of functionally graded 2-D cellular structures: a finite element simulation, Mater. Sci. Eng. A 499 (1–2) (2009) 434–439.
[8] D. Karagiozova, M. Alves, Propagation of compaction waves in cellular materials with continuously varying density, Int. J. Solids Struct. 71 (2015) 323–337.
[9] S.R. Reid, C. Peng, Dynamic uniaxial crushing of wood, Int. J. Impact Eng. 19 (1997) 531–570.
[10] P.J. Tan, S.R. Reid, J.J. Harrigan, Z. Zou, S. Li, Dynamic compressive strength properties of aluminum foams. Part II—'shock' theory and comparison with experimental data and numerical models, J. Mech. Phys. Solids 53 (2005) 2206–2230.
[11] Z.J. Zheng, Y.D. Liu, J.L. Yu, S.R. Reid, Dynamic crushing of cellular materials: continuum-based wave models for the transitional and shock modes, Int. J. Impact Eng. 42 (2012) 66–79.
[12] S. Pattofatto, I. Elnasri, H. Zhao, H. Tsitsiris, F. Hild, Y. Girard, Shock enhancement of cellular structures under impact loading: part II analysis, J. Mech. Phys. Solids 55 (12) (2007) 2671–2686.
[13] J.J. Harrigan, S.R. Reid, P.J. Tan, T.Y. Reddy, High rate crushing of wood along the grain, Int. J. Mech. Sci. 47 (4–5) (2005) 521–544.
[14] J.J. Harrigan, S.R. Reid, A.S. Yaghoubi, The correct analysis of shocks in a cellular material, Int. J. Impact Eng. 37 (8) (2010) 918–927.
[15] Z.J. Zheng, J.L. Yu, C.F. Wang, S.F. Liao, Y.D. Liu, Dynamic crushing of cellular materials: a unified framework of plastic shock wave models, Int. J. Impact Eng. 53 (2013) 29–43.
[16] Z.J. Zheng, C.F. Wang, J.L. Yu, S.R. Reid, J.J. Harrigan, Dynamic stress-strain states for metal foams using a 3D cellular model, J. Mech. Phys. Solids 72 (2014) 93–114.
[17] Y.Y. Ding, S.L. Wang, K. Zhao, Z.J. Zheng, L.M. Yang, J.L. Yu, Blast alleviation of cellular sacrificial cladding: a nonlinear plastic shock model, Int. J. Appl. Mech. 8 (4) (2016) 1650057.
[18] A.H. Brothers, D.C. Dunand, Mechanical properties of a density-graded replicated aluminum foam, Mater. Sci. Eng. A 489 (1–2) (2008) 439–443.
[19] Y. Hangai, K. Takahashi, R. Yamaguchi, T. Utsunomiya, S. Kitahara, O. Kuwazuru, N. Yoshikawa, Nondestructive observation of pore structure deformation behavior of functionally graded aluminum foam by X-ray computed tomography, Mater. Sci. Eng. A 556 (2012) 678–684.
[20] J. Zheng, Q.H. Qin, T.J. Wang, Impact plastic crushing and design of density-graded cellular materials, Mech. Mater. 94 (2016) 66–78.
[21] J.J. Zhang, Z.H. Wang, L.M. Zhao, Dynamic response of functionally graded cellular materials based on the Voronoi model, Compos. Part B Eng. 85 (2016) 176–187.
[22] A. Pollien, Y. Conde, L. Pambaguian, A. Mortensen, Graded open-cell aluminium foam core sandwich beams, Mater. Sci. Eng. A 404 (1–2) (2005) 9–18.
[23] Y. Matsumoto, A.H. Brothers, S.R. Stock, D.C. Dunand, Uniform and graded chemical milling of aluminum foams, Mater. Sci. Eng. A 447 (1–2) (2007) 150–157.
[24] A.F. Avila, Failure mode investigation of sandwich beams with functionally graded core, Compos. Struct. 81 (3) (2007) 323–330.
[25] S.A. Galehdari, M. Kadkhodayan, S. Hadidi-Moud, Low velocity impact and quasi-static in-plane loading on a graded honeycomb structure; experimental, analytical and numerical study, Aerosp. Sci. Technol. 47 (2015) 425–433.
[26] H.A. Bruck, A one-dimensional model for designing functionally graded materials to manage stress waves, Int. J. Solids Struct. 37 (2000) 6383–6395.
[27] S. Kiernan, L. Cui, M.D. Gilchrist, Propagation of a stress wave through a virtual functionally graded foam, Int. J. Non-Linear Mech. 44 (2009) 456–468.
[28] J.G. Liu, B. Hou, F.Y. Lu, H. Zhao, A theoretical study of shock front propagation in the density graded cellular rods, Int. J. Impact Eng. 80 (2015) 133–142.
[29] B. Yu, B. Han, P.B. Su, C.Y. Ni, Q.C. Zhang, T.J. Lu, Graded square honeycomb as sandwich core for enhanced mechanical performance, Mater. Des. 89 (2016) 642–652.
[30] C.J. Shen, G.X. Lu, T.X. Yu, Investigation into the behavior of a graded cellular rod under impact, Int. J. Impact Eng. 74 (2014) 92–106.
[31] X.K. Wang, Z.J. Zheng, J.L. Yu, Crashworthiness design of density-graded cellular metals, Theor. Appl. Mech. Lett. 3 (3) (2013) 031001.
[32] L. Cui, S. Kiernan, M.D. Gilchrist, Designing the energy absorption capacity of functionally graded foam materials, Mater. Sci. Eng. A 507 (1–2) (2009) 215–225.
[33] Y. Liu, H.X. Wu, B. Wang, Gradient design of metal hollow sphere (MHS) foams with density gradients, Compos. Part B: Eng. 43 (3) (2012) 1346–1352.
[34] A. Scholes, Railway passenger vehicle design loads and structural crashworthiness. Proceedings of the Institution of Mechanical Engineers, Part D: Journal of Automobile Engineering, 201(3), pp. 201–207, 1987.
[35] C.Gadd, Use of a weighted-impulse criterion for estimating injury hazard. No. 660793. SAE Technical Paper, 1966.
[36] X.K. Wang, Z.J. Zheng, J.L. Yu, C.F. Wang, Impact resistance and energy absorption of functionally graded cellular structures, Appl. Mech. Mater. 69 (2011) 73–78.
[37] S.L. Wang, Y.Y. Ding, C.F. Wang, Z.J. Zheng, J.L. Yu, Dynamic material parameters of closed-cell foams under high-velocity impact, Int. J. Impact Eng. 99 (2017) 111–121.
[38] Y.L. Sun, B. Amirrasouli, S.B. Razavi, Q.M. Li, T. Lowe, P.J. Withers, The variation in elastic modulus throughout the compression of foam materials, Acta Mater. 110 (2016) 161–174.
[39] L.L. Wang, Foundations of Stress Waves, Elsevier Science Ltd, Amsterdam, 2007.